Original Research Article

Tropical Journal of Chemistry, January 2025; 1(1): 17-25
Available online at http://www.tjchem.org

Antimicrobial activity of Synthesized Zinc Oxide-Carbonized Moringa Oleifera Leaf Nano Composite

*[1]Osahon Kennedy OGBEIDE, [1]Lawrence Ojong NDIP, [1]Oghenenyerhovwo Christabel UDEZI, [2]Gregory Esosa ONAIWU, [3]Ikhazuagbe Hilary IFIJEN

[1]*Department of Chemistry, University of Benin, Benin City, Edo State, Nigeria*
[2]*Department of Physical Sciences (Chemistry option), Benson Idahosa University, Benin City, Edo State, Nigeria*
[3]*Department of Research Outreach, Rubber Research Institute of Nigeria, Benin City, Edo State, Nigeria*
***Correspondent Author :** kennedy.ogbeide@uniben.edu

Article Information

Article history: Received December 2024
Revised December 2024
Accepted December 2024
Published online January 2025

ABSTRACT

Zinc oxide nanoparticles (ZnO NPs) are renowned for their biocompatibility and low toxicity, making them suitable for various biomedical applications. Moringa oleifera leaves, rich in minerals, vitamins, and phytochemicals, also exhibit notable antimicrobial potential. In this study, a Zinc Oxide-Carbonized Moringa oleifera (ZnO-CMO) nanocomposite was synthesized using the co-precipitation method and characterized via X-ray Diffraction (XRD), Fourier-Transform Infrared Spectroscopy (FT-IR), and Scanning Electron Microscopy (SEM). SEM analysis revealed a porous, finger-like morphology with uniform ZnO dispersion in the carbonized Moringa oleifera matrix, confirming successful composite formation. XRD patterns indicated high crystallinity, with ZnO as the dominant phase and average particle dimensions of approximately 36 nm. Antibacterial activity was evaluated at 250 mg/mL, showing differential inhibition profiles against various microorganisms. Staphylococcus aureus exhibited the highest susceptibility with a zone of inhibition (22.5 ± 1.0 mm), followed by *Escherichia coli* (14.5 ± 1.0 mm) and *Streptococcus* (12.0 ± 0.0 mm). In contrast, Pseudomonas displayed no measurable inhibition, likely due to resistance mechanisms like biofilm formation. Antifungal assays against Candida albicans and Aspergillus spp. showed no observable activity, suggesting limited efficacy against fungal pathogens. These results highlight the selective antibacterial potential of the ZnO-CMO nanocomposite, particularly against Gram-positive bacteria. Further optimization is needed to enhance its antifungal properties and broaden its antimicrobial spectrum. This study underscores the ZnO-CMO nanocomposite as a promising candidate for antibacterial applications and provides a foundation for future investigations to improve its efficacy.

Keywords: Nanocomposite**,** *moringa oleifera* leaf, coprecipitation, antimicrobial activity, zinc oxide.

1.0 INTRODUCTION

Nanotechnology has revolutionized numerous scientific disciplines, offering unprecedented avenues for innovation and transformative advancements. Central to this field is the utilization of nanoparticles (NPs)—materials with dimensions ranging between 1 and 100 nanometers. These nanoscale dimensions impart unique physicochemical properties, including a high surface area-to-volume ratio, quantum confinement effects, and enhanced reactivity [1–3]. Such properties significantly diverge from those of their bulk counterparts, facilitating groundbreaking applications across sectors such as electronics, energy, medicine, and environmental remediation [4–6]. Among the diverse classes of nanoparticles, metal oxide nanoparticles have emerged as particularly compelling due to their structural versatility, thermal stability, and extensive functional capabilities [7]. Within this category, zinc oxide nanoparticles (ZnO-NPs) have garnered widespread attention, owing to their remarkable properties, such as biocompatibility, cost-effectiveness, ease of synthesis, and environmental friendliness. ZnO-NPs exhibit high photosensitivity, a large excitation binding energy, excellent thermal conductivity, and outstanding

chemical stability, even under harsh environmental conditions. These attributes have propelled their adoption in various domains, particularly in biomedicine, where they serve as antimicrobial agents, wound-healing enhancers, drug delivery systems, and anti-cancer therapeutics [8–10]. Simultaneously, natural products have re-emerged as invaluable resources for the development of sustainable and bio-friendly materials. Among these, *Moringa oleifera*, commonly known as the drumstick tree, stands out as a resource of significant scientific interest. Native to South Asia and extensively cultivated in regions such as South Africa, the Philippines, Sudan, and Egypt, *Moringa oleifera* is celebrated for its nutritional, medicinal, and industrial applications. Belonging to the Moringaceae family, this fast-growing plant is rich in bioactive compounds such as flavonoids, phenolic acids, and vitamins, which confer potent antioxidant, antibacterial, anti-inflammatory, anti-cancer, and anti-diabetic properties. These attributes have positioned *Moringa oleifera* as a cornerstone in the food, pharmaceutical, and cosmetic industries [11–12].

The integration of ZnO-NPs with bio-derived materials like *Moringa oleifera* extracts offers a synergistic platform for the creation of advanced nanocomposites. Nanocomposites, defined as composite materials containing at least one nanoscale dimension, represent a paradigm shift in materials science. By combining the mechanical strength and functionality of reinforcing phases with the adaptability of matrix phases, nanocomposites deliver enhanced performance. Specifically, ZnO-NP–*Moringa oleifera*-based composites show great promise in addressing urgent biomedical challenges, such as the global rise of multidrug-resistant bacterial strains [13]. This alarming health crisis, exacerbated by the overuse and misuse of conventional antibiotics, underscores the need for alternative antimicrobial strategies.

In this context, *Moringa oleifera*'s inherent antimicrobial and antioxidant properties complement the biocidal activity of ZnO-NPs, yielding nanocomposites with superior therapeutic efficacy. Moreover, the carbonization of *Moringa oleifera* leaves further enhances their structural integrity and functional properties, making them highly suitable for integration into high-performance nanomaterials. By leveraging these complementary attributes, ZnO-NP–*Moringa oleifera* nanocomposites present a sustainable and effective approach to combating bacterial infections. This study focuses on the synthesis of zinc oxide-carbonized *Moringa oleifera* leaf nanocomposites and evaluates their antimicrobial activity. Through the investigation of physicochemical interactions between ZnO-NPs and bio-derived carbonized *Moringa oleifera*, this work aims to advance the development of novel, eco-friendly materials for biomedical applications. The findings have the potential to address critical challenges in healthcare, particularly in mitigating the impact of antibiotic-resistant pathogens.

2.0 MATERIALS AND METHODS

Zinc nitrate hexahydrate ($Zn(NO_3)_2{\cdot}6H_2O$), sodium hydroxide (NaOH), and polyvinyl alcohol (PVA) were purchased from Pyrex Chemical Company, Edo State, Nigeria. All chemicals and solvents used were of analytical grade and were utilized without further purification. Moringa oleifera leaves were collected directly from the tree, thoroughly rinsed with running water, and air-dried for two days. Subsequently, the leaves were oven-dried at 100°C for 20 minutes and sterilized before being ground using a British milling machine. The powdered leaves were carbonized in a muffle furnace at 350°C for 40 minutes and allowed to cool for one hour to prevent oxidation upon exposure to air. The carbonized leaves were then further ground using a mortar and pestle to achieve a finer texture and sieved using a 250 µm sieve to isolate fine particles. The resulting filtrate was stored in an airtight container to prevent contamination, while the residue was set aside for other potential uses.

2.1 Preparation of Zinc Oxide-Carbonized Moringa Oleifera Nanocomposite

The synthesis of **Zinc Oxide-Carbonized Moringa Oleifera Nanocomposite** was conducted using the co-precipitation method described by Ghorbani and others [14].

2.1.1 Preparation of Standard Solutions

A known quantity of zinc nitrate hexahydrate (10.00 g) was accurately weighed and dissolved in approximately 500 mL of distilled water to ensure complete dissolution. The solution was then transferred into a 1000 mL volumetric flask. Separately, a specific amount of polyvinyl alcohol (PVA), such as 2.00 g, was weighed and dissolved in 200 mL of distilled water. The mixture was gently heated while stirring to ensure complete dissolution. Once dissolved, the PVA solution was added to the zinc nitrate solution in the volumetric flask. Similarly, a measured amount of sodium hydroxide (4.00 g) was dissolved in 300 mL of distilled water in a separate volumetric flask. This solution was combined with an additional portion of PVA solution (50 mL) and mixed thoroughly. Finally, all solutions were topped up to the 1000 mL mark with distilled water, ensuring uniform concentrations of the standard solutions.

2.1.2 Synthesis Process

A magnetic stirrer, retort stand, and burette were set up for synthesis. Sodium hydroxide solution was placed in the burette, while the zinc nitrate solution was added to a conical flask on the magnetic stirrer. Sodium hydroxide was gradually added dropwise over one hour with continuous stirring at 30°C and 1500 rpm. Afterwards, carbonised 0.1g Moringa oleifera was weighed and incorporated into the solution while stirring continuously for 30 minutes. This procedure

was repeated 11 times. The resulting solution underwent centrifugation to separate the solid phase from the liquid. The supernatant was discarded, and the pellet was collected and transferred to a crucible. Calcination was performed at 250°C for 40 minutes to remove impurities, the PVA stabilizer, and excess water. The calcined sample, which appeared grey, loose, and dispersible, was finely ground and stored in a sample container for further analysis.

2.2 Source of Microorganisms

The microorganisms used in this study, including *Candida albicans*, *Staphylococcus aureus*, *Escherichia coli*, *Streptococcus pyogenes*, *Pseudomonas aeruginosa*, and *Aspergillus flavus*, were clinical isolates procured from the University of Benin Teaching Hospital, Benin City. The isolates were collected in sterile containers and characterized based on their cultural and morphological properties.

2.3 Preparation of Agar

Mueller Hinton agar was prepared by dissolving 3.8 g of Mueller Hinton powder in 1000 mL of distilled water, followed by sterilization in an autoclave at 120°C for 15 minutes. The agar was allowed to cool and mixed thoroughly before being poured into Petri dishes and left to solidify.

2.4 Preparation of Stock Solutions

A ciprofloxacin stock solution (0.5 mg/mL) was prepared using a 10% DMSO solution. Similarly, a stock solution of the synthesized sample was prepared by dissolving 1.0 g of the sample in 3 mL of a 20% DMSO solution.

2.5 Antimicrobial Susceptibility Tests

The antimicrobial assay was conducted using a modified ditch-plate technique. Molten agar was poured into sterile Petri dishes and allowed to solidify. A 6-mm diameter ditch was created in the solidified agar using a sterile cork borer, and the ditch base was sealed with molten Mueller Hinton agar. After solidification, test organisms were streaked radially onto the agar surface using a loopful of previously diluted cultures. The synthesized nanocomposite solution was carefully pipetted into the ditch, filling it to three-quarters of its capacity.

Organisms resistant to the sample grew up to the edge of the ditch, while susceptible organisms exhibited a zone of inhibition. All experiments were performed in duplicate. Plates were incubated at 37°C for 18–24 hours, and the width of the inhibition zones was measured using a digital calliper to assess the relative antimicrobial activity of the sample.

2.6 Determination of Antibacterial Activity

The antibacterial activity of the synthesized nanocomposite was evaluated using the agar well diffusion method, following the protocol by Irfan and others [15].

Gram-positive (*Staphylococcus aureus*, *Bacillus subtilis*) and Gram-negative (*Escherichia coli*, *Pseudomonas aeruginosa*) bacteria were cultured on nutrient agar slants. Fresh cultures were prepared by inoculating bacterial strains into nutrient broth and incubating at 37°C for 18–24 hours. The nanocomposite solution was prepared at 250 mg/mL in sterile distilled water and vortexed to ensure uniform dispersion.

Mueller Hinton agar plates were seeded with 100 µL of microbial suspension adjusted to the 0.5 McFarland standard. Wells (6 mm in diameter) were punched into the agar, and 100 µL of the nanocomposite solution was added to each well. Negative controls included sterile distilled water, while ciprofloxacin served as the positive control. Plates were incubated at 37°C for 24 hours. Zones of inhibition were measured in triplicate to ensure accuracy and reliability.

2.7 Characterization of Synthesized Zinc Oxide-Carbonized Moringa Oleifera Leaf Nanocomposite

The nanoparticles (NPs) undergo comprehensive physiochemical characterization to evaluate their size, shape, functional groups, and purity, utilizing several advanced techniques, including Scanning Electron Microscopy (SEM), Fourier Transform Infrared Spectroscopy (FTIR), and X-ray Diffraction (XRD). These techniques are commonly employed for both structural and chemical characterization of nanomaterials. X-ray Diffraction (XRD) was employed to determine the crystalline structure and phase identification of the zinc oxide nanocomposite. A Rigaku Mini Flex 600, manufactured by Rigaku Corporation, Japan, was used for XRD analysis. The system was operated with a tube voltage of 40 kV and a current of 15 mA, utilizing a 2θ scanning range from 5° to 70° and a scan rate of 2° per minute. Fourier Transform Infrared Spectroscopy (FTIR) was utilized to identify the chemical groups and bonding present within the nanocomposite. A Cary 360 FTIR spectrometer (Agilent Technologies Inc., USA) was used to obtain the FTIR spectra of the sample. The samples were scanned 16 times in the range of 4000 cm^{-1} to 400 cm^{-1}, with a resolution of 4 cm^{-1}, optical velocity of 0.4747, and an aperture of 100. The resulting spectrum provides detailed information about the functional groups present in the sample across the specified wavelength range. Scanning Electron Microscopy (SEM) was used to examine the surface morphology of the synthesized zinc oxide nanoparticles (ZnO-NP) impregnated in carbonated Moringa oleifera. A JOEL-JSM 7600F scanning electron microscope was employed for this analysis. A small sample was placed on carbon tape and gold-coated to enhance conductivity. The sample was then placed on a movable stage under a vacuum, and the surface was scanned using an electron beam. This technique provided high-resolution images of the sample at 8,000x, 9,000x, and 10,000x magnifications. The SEM images, presented in black and white, offer detailed

visual information about the nanocomposite's surface structure and morphology.

3.0 RESULTS AND DISCUSSION

3.1 Fourier-Transform Infrared (FTIR) Spectrum Analysis

The Fourier-transform infrared (FTIR) spectrum of the Zinc Oxide-Carbonized Moringa Nanocomposite (ZnO-CMO) was analyzed to identify the characteristic functional groups present in the material. In the spectrum (Fig.1), distinct absorption bands were observed at specific wavenumbers,

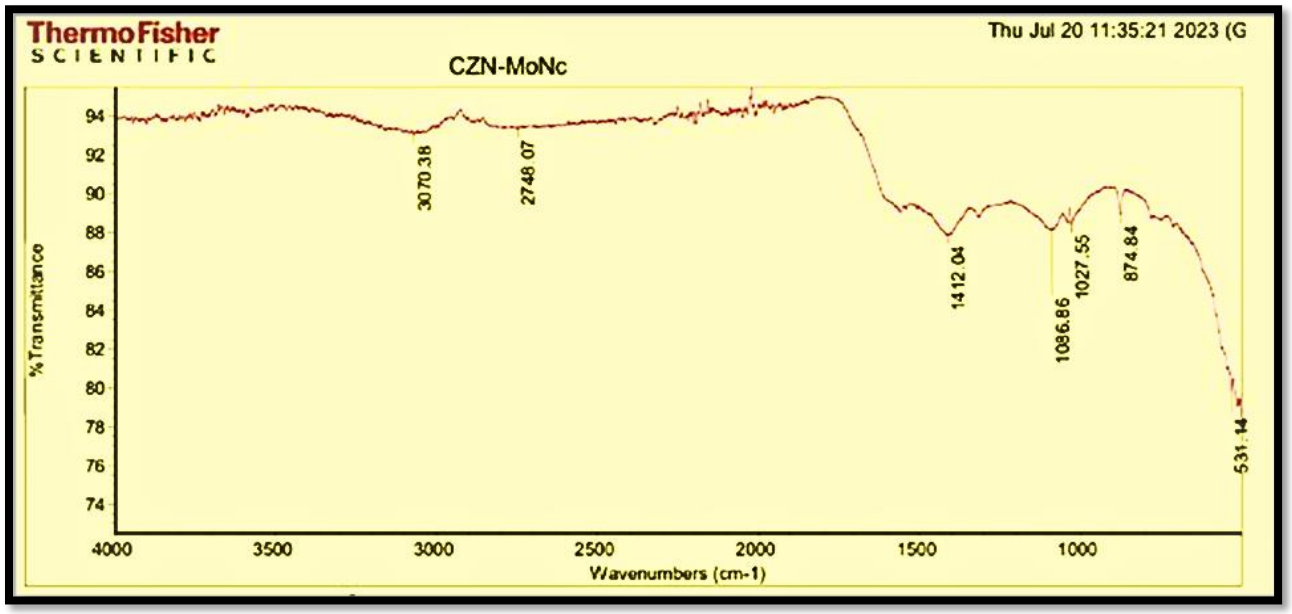

Figure 1: Fourier-transform infrared (FTIR) spectrum of Zinc Oxide-Carbonized Moringa Nanocomposite (ZnO-CMO)

indicating the presence of various functional groups.

The absorption band at 3070.38 cm^{-1} corresponds to OH stretching vibrations, suggesting the presence of hydroxyl groups, typically associated with alcohols (Figure 1). This band was weak and broad, indicating a relatively low concentration of hydroxyl groups in the nanocomposite [16]. Similarly, the absorption band at 2748.07 cm^{-1}, also weak and broad, indicates another OH stretching vibration, supporting the presence of hydroxyl groups in the material. In the functional group region (4000–1500 cm^{-1}), an absorption band at 1412.04 cm^{-1} was observed, corresponding to OH bending vibrations characteristic of carboxylic acid functional groups. This band had medium intensity, indicating a moderate concentration of carboxylic acid groups in the ZnO-CMO nanocomposite [17–18]. Additionally, a distinct absorption band at 531.14 cm^{-1} in the fingerprint region (1400–400 cm^{-1}) signifies the presence of metallic oxide, specifically zinc oxide. This observation confirms the successful incorporation of zinc oxide nanoparticles into the presence of carbonized Moringa within the nanocomposite, consistent with the synthesis process. The presence of Zinc (15.60%) confirms the incorporation of Zinc Oxide (ZnO) into the nanocomposite. ZnO is known for its various composite structure [18]. Overall, the FTIR analysis provides valuable insights into the composition and functional groups of the ZnO-CMO nanocomposite, contributing to a better understanding of its properties and potential applications.

3.2 Energy-dispersive X-ray Spectroscopy (EDX) Analysis.

Energy-dispersive X-ray spectroscopy (EDX) was employed to determine the elemental composition of the Zinc Oxide-Carbonized Moringa Nanocomposite (ZnO-CMO). The results (Figure 2) are expressed in weight percentage, revealing the relative abundance of each element within the material. The composition is expressed in weight percentage, indicating the relative abundance of each element within the nanocomposite. Oxygen is found to be the most prevalent element, constituting 20.40% of the composite's composition. This is expected, as oxygen is commonly found in oxides and organic compounds. Carbon, comprising 56.15% of the composition, suggests a significant

applications in electronics, optics, and medicine due to its unique properties. Additionally, the detection of Molybdenum (3.42%) indicates a possible additive or impurity introduced during the synthesis process. Molybdenum has various industrial applications,

including being an alloying agent and catalyst in steel production. Potassium (1.21%) and Aluminum (3.22%) were also detected in the nanocomposite, albeit in smaller percentages (Figure 2). These elements may originate from precursor materials, reaction intermediates, or contaminants introduced during the synthesis process. The presence of potassium suggests the possible use of potassium-containing compounds or reagents during synthesis. Similarly, aluminium could be present as an impurity in the precursor materials or from the experimental setup.Overall, the EDX analysis provides valuable insights into the elemental composition of the ZnO-CMO nanocomposite. The detected elements corroborate with the expected constituents based on the synthesis process. However, the presence of minor elements such as molybdenum, potassium, and aluminium indicates the possibility of impurities or additives, which may warrant further investigation. Further characterisation techniques, such as X-ray diffraction (XRD) and scanning electron microscopy (SEM), can provide additional information about the nanocomposite's structure, morphology, and purity.

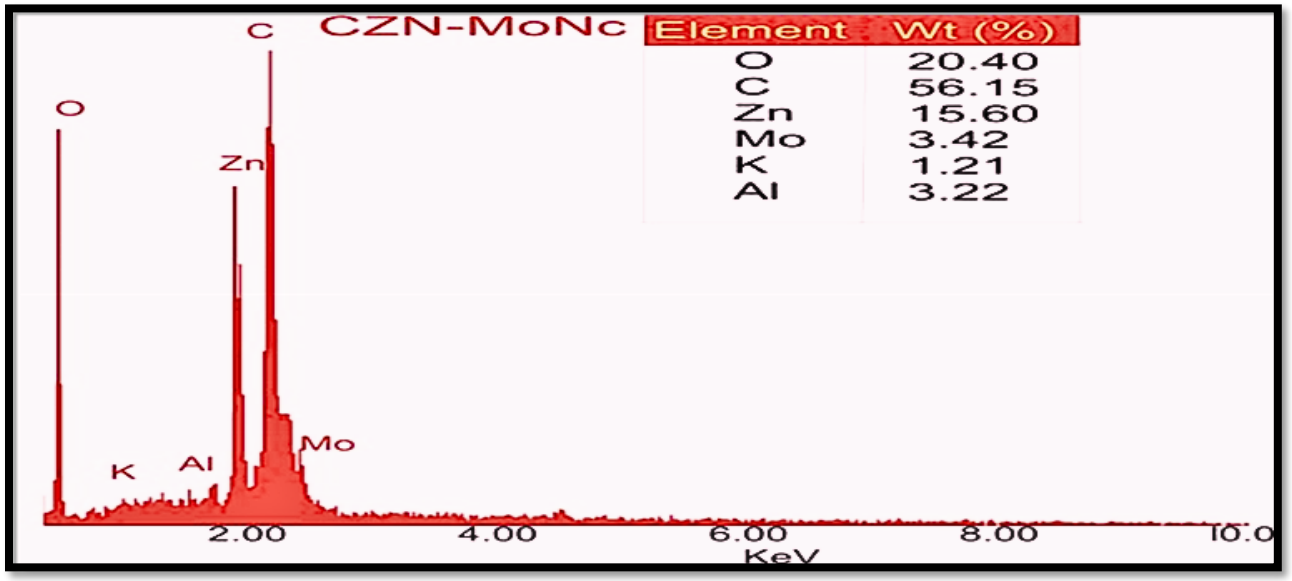

Figure 2: EDX of Zinc Oxide-Carbonized Moringa Nanocomposite (ZnO-CMO)

3.3 Scanning Electron Microscopy (SEM) Analysis

Figure 3 shows the SEM image of the Zinc Oxide - Carbonized Moringa Nanocomposite (ZnO-CMO). Scanning Electron Microscopy (SEM) analysis of the ZnO-CMO nanocomposite revealed a highly porous microstructure, which plays a pivotal role in its antimicrobial efficacy. This porosity significantly enhances the composite's surface area, allowing for increased interactions with microbial cells. The intricate porous network promotes microbial adhesion and retention, facilitating close contact necessary for effective antimicrobial activity. The integration of zinc oxide within the carbonized *Moringa oleifera* matrix contributes to the composite's potent bactericidal and fungicidal properties. The porous architecture maximizes the exposure of zinc oxide particles to microorganisms, thereby enhancing the generation of reactive oxygen species (ROS) and the disruption of microbial membranes and metabolic processes. Furthermore, the synergistic interaction between the bioactive compounds inherent in *Moringa oleifera* and the antimicrobial capabilities of zinc oxide amplifies the composite's efficacy. This synergy likely results from combined oxidative stress mechanisms and additional antimicrobial phytochemicals contributed by the carbonized matrix. Such a composite structure is highly advantageous for practical applications, including wound healing, water purification, and antimicrobialsurface coatings, offering a multifunctional approach to addressing microbial challenges.

.

Figure 3: SEM of Zinc Oxide-Carbonized Moringa Nanocomposite (ZnO-CMO)

3.4 X-ray Diffraction (XRD) Analysis

Figure 4 illustrates the X-ray Diffraction (XRD) pattern of the Zinc Oxide-Carbonized Moringa Nanocomposite (ZnO-CMO). XRD analysis revealed diffraction peaks corresponding to both zinc oxide and carbonized Moringa Oleifera phases. Peaks for ZnO included (100), (002), (101), (102), (110), (103), (200), (201), (202), and (112), while carbonized Moringa Oleifera peaks were observed at (002), (004), (100), and (101) [19–21]. The dominance of ZnO peaks indicates it as the primary phase in the composite. The sharp and well-defined peaks confirm high crystallinity, essential for photocatalysis and antimicrobial activity.

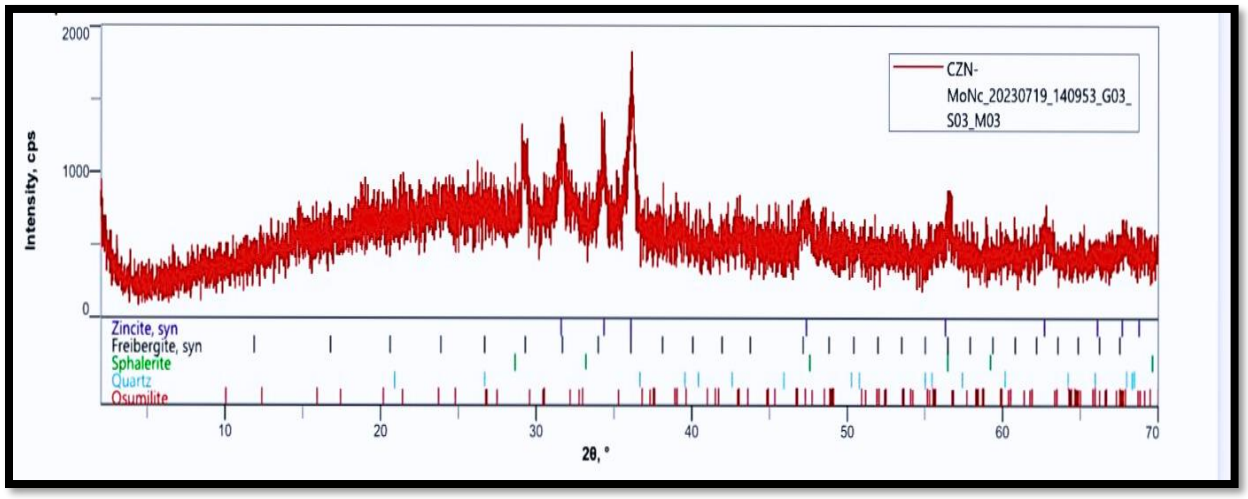

Figure 4: X-ray Diffraction (XRD) of ZnO-CMO

3.5 Antimicrobial Activity of Zinc Oxide-Carbonized Moringa Nanocomposite

3.5.1 Antibacterial Activity

Table 1 presents the antibacterial potential of the *zinc oxide-carbonized Moringa nanocomposite*, which was

evaluated against various bacterial strains, showcasing a differential inhibition profile. The *inhibition zones*, measured in millimeters at a concentration of *250 mg/mL*, provide a quantitative measure of the nanocomposite's antimicrobial activity, illustrating its effectiveness against both *Gram-positive* and *Gram-negative bacteria*.

Escherichia coli, a *Gram-negative bacterium*, exhibited a moderate *inhibition zone* of *14.5 ± 1.0 mm*. This finding indicates a significant antibacterial effect, likely arising from the nanocomposite's interaction with the bacterial cell wall or membrane. Potential mechanisms include the generation of *reactive oxygen species (ROS)* or the disruption of bacterial metabolic processes. However, the relatively moderate inhibition observed for *E. coli* may also be attributed to the structural defense provided by the *Gram-negative outer membrane*, which serves as a barrier against nanoparticle penetration and reduces susceptibility to antimicrobial agents.

In contrast, *Staphylococcus aureus*, a *Gram-positive bacterium*, showed the highest *inhibition zone* of *22.5 ± 1.0 mm*, demonstrating its heightened susceptibility to the nanocomposite. The structural simplicity of *Gram-positive bacteria*, lacking an *outer membrane*, allows *zinc oxide nanoparticles* to penetrate and interact more readily with the *peptidoglycan-rich cell wall*. This interaction may intensify oxidative stress via *ROS generation*, leading to significant bacterial damage. Additionally, the *carbonized Moringa* component in the composite likely contributes synergistically, enhancing the antibacterial activity through its inherent antimicrobial phytochemicals [22-23].

Pseudomonas, another *Gram-negative bacterium*, exhibited no measurable *inhibition zone*, indicating resistance to the nanocomposite at the tested concentration. This resistance is likely due to the bacterium's robust defense mechanisms, including *efflux pumps* that actively expel nanoparticles, *biofilm formation* that shields bacterial cells, and enzymatic degradation of *reactive species*. The absence of measurable activity against *Pseudomonas* underscores the challenges in targeting certain *Gram-negative pathogens* with nanoparticle-based composites and highlights the need for further refinement of the composite's properties to overcome these barriers.

Streptococcus, a *Gram-positive bacterium*, displayed an *inhibition zone* of *12.0 ± 0.0 mm*. While this is smaller than that observed for *Staphylococcus aureus*, it confirms the nanocomposite's antibacterial activity against another *Gram-positive strain*. The absence of standard deviation in the *inhibition zone* measurement suggests a consistent and reproducible effect, reflecting the stability of the interaction between the nanocomposite and the bacterial cells.

These findings underscore the selective efficacy of the *zinc oxide-carbonized Moringa nanocomposite*, particularly against *Gram-positive bacteria*. The differences in *inhibition zones* among the tested microorganisms are likely influenced by the structural and biochemical characteristics of their cell walls. The greater effectiveness against *Gram-positive bacteria* highlights the advantage of nanoparticle-based composites in penetrating *peptidoglycan-rich cell walls*, whereas the resistance of *Gram-negative bacteria* emphasizes the need for strategic enhancements to target their protective *outer membranes*. Overall, the results provide a promising foundation for further optimization of the nanocomposite to enhance its broad-spectrum antibacterial activity and address resistance in *Gram-negative bacteria*.

Table 1: Antibacterial potential zinc oxide-carbonized moringa nanocomposite

Microorganism	Inhibition Zone (mm)	S.D.
Escherichia coli	14.5	± 1.0
Staphylococcus aureus	22.5	± 1.0
Pseudomonas	Null	
Streptococcus	12.0	± 0.0

SD: Standard deviation

3.5.2 Antifungal Activity

Table 2 presents the antifungal potential of the zinc oxide-carbonized Moringa nanocomposite (ZnO-CMO). The antifungal potential of the zinc oxide-carbonized Moringa nanocomposite was assessed against *Candida albicans* and *Aspergillus* but revealed no observable inhibitory activity under the tested conditions. This result highlights the composite's limited efficacy against these fungal strains, suggesting that its antifungal properties are either negligible or insufficient to significantly disrupt fungal growth. The absence of activity underscores the specificity of the composite's antimicrobial mechanisms, which appear to be more effective against bacterial pathogens than fungal species.

Candida albicans, a prevalent opportunistic fungal pathogen, is known for its resilience and ability to form biofilms. These biofilms enhance resistance to various antimicrobial agents by creating a protective extracellular matrix that inhibits the penetration and efficacy of antimicrobial compounds. The lack of inhibitory activity against *Candida albicans* suggests that the nanocomposite may fail to generate adequate reactive oxygen species (ROS) or to disrupt critical structural components, such as the fungal cell wall or membrane. These mechanisms are essential for effective antifungal action. Alternatively, this result could indicate that the composite's physicochemical properties are optimized for interactions with bacterial

rather than fungal cells, which have distinct structural and biochemical characteristics.

Similarly, the absence of activity against *Aspergillus*, a filamentous fungus, suggests that the composite does not interfere effectively with its growth processes. The robust cell wall structure of *Aspergillus*, predominantly composed of chitin and glucans, may resist the mechanisms of action of the composite, such as ROS generation or membrane disruption. Furthermore, *Aspergillus* species are known for their inherent antifungal resistance mechanisms, including the presence of efflux pumps and enzymatic degradation of reactive agents. These defense strategies could contribute to the null result observed in this study.

The lack of detectable antifungal activity for both *Candida albicans* and *Aspergillus* emphasizes the specificity of the zinc oxide-carbonized Moringa nanocomposite towards bacterial pathogens. This specificity suggests that the composite's current formulation is insufficient for antifungal applications, necessitating further optimization to broaden its antimicrobial spectrum. Future research could focus on enhancing the composite's antifungal efficacy by increasing the concentration of active components, incorporating synergistic antifungal agents, or tailoring the surface chemistry to improve interactions with fungal cell walls. These adjustments could potentially overcome the structural and biochemical barriers posed by fungal cells, enabling more effective inhibition of fungal growth. While the composite demonstrates significant antibacterial activity, its antifungal efficacy remains undetectable against the tested fungal strains. This limitation underscores the importance of targeted modifications to the composite's formulation, paving the way for its potential application as a broad-spectrum antimicrobial agent.

Table 2: Antifungal Potential of ZnO-CMO

Microorganism	Inhibitory Activity
Candida albicans	Null
Aspergillus	Null

Conclusion

The successful synthesis of the zinc oxide-carbonized *Moringa oleifera* leaf nanocomposite highlights its significant antimicrobial activity against both Gram-positive and Gram-negative bacteria. This efficacy stems from the synergistic effects of zinc oxide nanoparticles, which generate reactive oxygen species and release antimicrobial zinc ions, and bioactive phytochemicals from the carbonized *Moringa oleifera* leaf extract, which enhance membrane disruption and enzymatic inhibition. These properties position the nanocomposite as a promising material for applications such as antimicrobial wound dressings, medical device coatings, and drug delivery systems. However, further studies are needed to elucidate its precise mechanisms of action, assess long-term toxicity, and validate its safety and efficacy in clinical settings. With continued research, this nanocomposite holds significant potential to address antimicrobial resistance and improve infection control in various biomedical applications.

Acknowledgements: We extend our heartfelt gratitude to everyone who contributed to the success of this paper. In particular, we wish to acknowledge the technologists at the Chemistry Department, University of Benin, for their invaluable assistance. Your support is deeply appreciated, and we remain eternally grateful.

References

[1] Liu, Q., Zhang, A., Wang, R., Zhang, Q., & Cui, D. (2021). A Review on Metal- and Metal Oxide-Based Nanozymes: Properties, Mechanisms, and Applications. *Nano-Micro Letters*, 13. https://doi.org/10.1007/s40820-021-00674-8.

[2] Okonkwo, T. P., Amienghemhen, O. D., Nkwor, A. N., & Ifijen, I. H. (2024). Exploring the versatility of copper-based nanoparticles as contrast agents in various imaging modalities. *Nano-Structures & Nano-Objects, 40*, 101370. https://doi.org/10.1016/j.nanoso.2024.101370.

[3] Mendes, P., Song, Y., W., Gani, T., Lim, K., Kawi, S., & Kozlov, S. (2023). Opportunities in the design of metal@oxide core-shell nanoparticles. *Advances in Physics: X*, 8. https://doi.org/10.1080/23746149.2023.2175623.

[4] Onivefu, A. P., Ikhuoria, E. U., Muniratu, M., et al. (2024). Exploring the remarkable gas sensing capability of molybdenum diselenide nanoparticles. In *TMS 2024 153rd Annual Meeting & Exhibition Supplemental Proceedings*. TMS 2024. *The Minerals, Metals & Materials Series.* Springer, Cham. https://doi.org/10.1007/978-3-031-50349-8_3.

[5] Mao, Y., & Gupta, S. (2022). Metal Oxide Nanomaterials: From Fundamentals to Applications. *Nanomaterials*, 12. https://doi.org/10.3390/nano12234340.

[6] Omoruyi, I. C., Omoruyi, J. I., Aghedo, O. N., Archibong, U. D., et al. (2023). Application of magnetic iron oxide nanostructures in drug delivery: A compact review. In *TMS 2023 152nd Annual Meeting & Exhibition Supplemental Proceedings. TMS 2023. The Minerals, Metals & Materials Series*. Springer, Cham. https://doi.org/10.1007/978-3-031-22524-6_22.

[7] Ikhuoria, E. U., Uwidia, I. E., Okojie, R. O., Ifijen, I. H., & Chikaodili, I. D. (2024). Prospects of utilizing environmentally friendly iron oxide nanoparticles synthesized from *Musa paradisiaca* extract for potential COVID-19 treatment. In *TMS 2024 153rd Annual Meeting & Exhibition Supplemental Proceedings. TMS 2024. The Minerals, Metals &*

Materials Series. Springer, Cham. https://doi.org/10.1007/978-3-031-50349-8_116.

[8] Jiang, J., Pi, J., & Cai, J. (2018). The Advancing of Zinc Oxide Nanoparticles for Biomedical Applications. *Bioinorganic Chemistry and Applications*, 2018. https://doi.org/10.1155/2018/1062562.

[9] Sruthi, S., Ashtami, J., & Mohanan, P. (2018). Biomedical application and hidden toxicity of Zinc oxide nanoparticles. *Materials Today Chemistry*. https://doi.org/10.1016/J.MTCHEM.2018.09.008.

[10] Murali, M., Kalegowda, N., Gowtham, H., Ansari, M., Alomary, M., Alghamdi, S., Shilpa, N., Singh, S., Thriveni, M., Aiyaz, M., Angaswamy, N., Lakshmidevi, N., Adil, S., Hatshan, M., & Amruthesh, K. (2021). Plant-Mediated Zinc Oxide Nanoparticles: Advances in the New Millennium towards Understanding Their Therapeutic Role in Biomedical Applications. *Pharmaceutics*, 13. https://doi.org/10.3390/pharmaceutics13101662.

[11] Pareek, A., Pant, M., Gupta, M., Kashania, P., Ratan, Y., Jain, V., Pareek, A., & Chuturgoon, A. (2023). Moringa oleifera: An Updated Comprehensive Review of Its Pharmacological Activities, Ethnomedicinal, Phytopharmaceutical Formulation, Clinical, Phytochemical, and Toxicological Aspects. *International Journal of Molecular Sciences*, 24. https://doi.org/10.3390/ijms24032098.

[12] Prajapati, C., Ankola, M., Upadhyay, T., Sharangi, A., Alabdallah, N., Al-Saeed, F., Muzammil, K., & Saeed, M. (2022). Moringa oleifera: Miracle Plant with a Plethora of Medicinal, Therapeutic, and Economic Importance. *Horticulturae*. https://doi.org/10.3390/horticulturae8060492.

[13] Gobinath, P., Packialakshmi, P., Ali, D., Alarifi, S., Gurusamy, R., Idhayadhulla, A., & Surendrakumar, R. (2022). Nanobased Antibacterial Drug Discovery to Treat Skin Infections of Staphylococcus aureus Using Moringa oleifera-Assisted Zinc Oxide Nanoparticle and Molecular Simulation Study. *BioMed Research International*, 2022. https://doi.org/10.1155/2022/7228259.

[14] Ghorbani, H. R., Mehr, F. P., Pazoki, H., & Rahmani, B. M. (2015). Synthesis of ZnO nanoparticles by precipitation method. *Oriental Journal of Chemistry, 31*(2). Retrieved from http://www.orientjchem.org/?p=8621.

[15] Irfan, M., Munir, H., & Ismail, H. (2021). Moringa oleifera gum based silver and zinc oxide nanoparticles: green synthesis, characterization and their antibacterial potential against MRSA. *Biomaterials Research*, 25. https://doi.org/10.1186/s40824-021-00219-5.

[16] Matinise, N., Fuku, X., Kaviyarasu, K., Mayedwa, N., & Maaza, M. (2017). ZnO nanoparticles via Moringa oleifera green synthesis: Physical properties & mechanism of formation. *Applied Surface Science*, 406, 339-347. https://doi.org/10.1016/J.APSUSC.2017.01.219.

[17] Durai, V., Kumar, E., & Indira, R. (2024). Green route to prepare zinc oxide nanoparticles using Moringa oleifera leaf extracts and their structural, optical and impedance spectral properties. *Semiconductor Physics, Quantum Electronics and Optoelectronics*. https://doi.org/10.15407/spqeo27.01.064.

[18] Sebastian, N., Yu, W., & Balram, D. (2020). Synthesis of amine-functionalized multi-walled carbon nanotube/3D rose flower-like zinc oxide nanocomposite for sensitive electrochemical detection of flavonoid morin. *Analytica chimica acta*, 1095, 71-81. https://doi.org/10.1016/j.aca.2019.10.026.

[19] Matinise, N., Fuku, X., Kaviyarasu, K., Mayedwa, N., & Maaza, M. (2017). ZnO nanoparticles via Moringa oleifera green synthesis: Physical properties & mechanism of formation. *Applied Surface Science*, 406, 339-347. https://doi.org/10.1016/J.APSUSC.2017.01.219.

[20] Durai, V., Kumar, E., & Indira, R. (2024). Green route to prepare zinc oxide nanoparticles using Moringa oleifera leaf extracts and their structural, optical and impedance spectral properties. *Semiconductor Physics, Quantum Electronics and Optoelectronics*. https://doi.org/10.15407/spqeo27.01.064.

[21] Irfan, M., Munir, H., & Ismail, H. (2021). Moringa oleifera gum-based silver and zinc oxide nanoparticles: green synthesis, characterization and their antibacterial potential against MRSA. *Biomaterials Research*, 25. https://doi.org/10.1186/s40824-021-00219-5.

[22] Ogbeide, O., Akhigbe, I. U., Unuigbe, C. A., Gabriel, B. O., & Erharuyi, O. (2023). Histological assessment and antimicrobial investigation of pure compound; 3,5,6,7-tetrahydroxy-19-vouacanoic acid; (3β, 5α, 6β, 7β)-form, 6,7-dibenzoyl (Pulcherrimin A) isolated from *Caesalpinia pulcherrima* stem bark. *Tropical Journal of Phytochemistry and Pharmaceutical Sciences, 2*(1). https://doi.org/10.26538/tjpps/v2i1.1.

[23] Aghedo, O. N., & Ogbeide, O. K. (2022). Proximate composition, acute toxicity, and antimicrobial activity of methanol extract of *Picralima nitida* stem bark. *ChemSearch Journal, 13*(2), 92–98. Publication of Chemical Society of Nigeria, Kano Chapter. Retrieved from http://www.ajol.info/index.php/csj